

Refereed, biannual scientific journal issued by: The Libyan Center for Solar Energy Research and Studies



Improving PEM Water Electrolysis Efficiency with ANN-Based Control to Handle Rapid Photovoltaic Power Fluctuations

Abdellah El Idrissi^{1*}, Belkasem Imodane², Hamid Hamdani³, M'hand Oubella⁴, Mohamed Benydir⁵, Mohamed Ajaamoum⁶.

1,2,4,5,6 Laboratory of Engineering Sciences and Energy Management (LASIME), Ibn Zohr University, National School of Applied Sciences, Agadir, Morocco.

³Engineering and Applied Physics Team (EAPT), Higher School of Technology, Sultan Moulay Slimane University, Beni Mellal, Morocco.

E-mail: ¹abdellah.elidrissi@edu.uiz.ac.ma ,²b.imodane@uiz.ac.ma ,³h.hamdani@usms.ma , ⁴m.oubella@uiz.ac.ma , ⁵ mohamed.benydir@edu.uiz.ac.ma , 6m.ajaamoum@uiz.ac.ma.

SPECIAL ISSUE ON:

The 1st International Conference on Sciences and Techniques for Renewable Energy and the Environment.

(STR2E 2025)

May 6-8, 2025 at FST-Al Hoceima-Morocco.

KEYWORDS

Hydrogen production,
Renewable energy, PEM
electrolyzer, DC-DC
Converter, Artificial Neural
Network.

ABSTRACT

This research presents an innovative method for enhancing hydrogen production through proton exchange membrane (PEM) water electrolysis, powered by photovoltaic (PV) energy. The system is based on the Perturbation and Observation (P & O) method of Maximum Power Point Tracking (MPPT) with a boost converter to maximize energy capture, and a buck converter to stabilize DC voltage, ensuring compatibility with the proton exchange membrane electrolyzer. An artificial neural network (ANN)-based controller manages the buck converter, effectively minimizing the effects of solar irradiation fluctuations on electrolyzer performance.

By using the adaptive learning capabilities of the ANN, the proposed approach increases the efficiency of hydrogen production under varying solar energy levels. Simulation results indicate that the ANN controller outperforms the conventional PI controller, reducing the mean absolute percentage error (MAPE) from 1.22 % to 0.95 %, decreasing overshoot from 12.84 % to 3.19 %, and achieving a faster settling time of 0.022 s compared to 0.023 s. This study advances renewable hydrogen production technologies, demonstrating that ANN-based control improves dynamic performance and contributes to the development of smarter, more resilient energy systems.

تحسين كفاءة التحليل الكهربائي للماء بتقنية الغشاء البروتوني (PEM) عبر التحكم القائم على الشبكات العصبية الاصطناعية لمواجهة التقلبات السريعة في الطاقة الكهربائية المولدة من الألواح الشمسية

عبد الله الإدريسي، بلقاسم اموضان، حميد حمداني، محند أوبلا، محمد بنيدير ، محمد اجعموم.

ملخص: يقدم هذا البحث طريقة مبتكرة لتحسين إنتاج الهيدروجين من خلال التحليل الكهربائي للماء باستخدام غشاء تبادل البروتون، مدعومًا بالطاقة الكهروضوئية. يستفيد النظام من طريقة التشويش القابلة والمرنة لتتبع نقطة القدرة القصوى مع محول تعزيز لزيادة التقاط الطاقة إلى أقصى حد، ومحول باك لتثبيت جهد التيار المستمر، مما يضمن التوافق مع المحلل الكهربائي بغشاء تبادل البروتون. يدير نظام تحكم قائم على الشبكة العصبية الاصطناعية محول باك، مما يقلل بشكل فعال من آثار تقلبات الإشعاع الشمسي على أداء المحلل الكهربائي.

من خلال الاستفادة من القدرة التعلمية التكيفية لنظام التحكم القائم على الشبكة العصبية الاصطناعية، يزيد النهج المقترح من كفاءة إنتاج الهيدروجين في ظل مستويات طاقة شمسية متفاوتة. تشير نتائج المحاكاة إلى أن وحدة تحكم النظام القائم على الشبكة العصبية الاصطناعية تتفوق على وحدة التحكم التناسبي التكاملي التقليدية، مما يوفر أوقات استجابة أسرع ويعزز كفاءة النظام. تعمل هذه الدراسة على تطوير تقنيات إنتاج الهيدروجين المتجددة، مما يدعم تطوير أنظمة طاقة أكثر ذكاءً ومرونة.

الكلمات المفتاحية – إنتاج الهيدروجين، الطاقة المتجددة، المحلل الكهربائي، محول التيار المستمر، الشبكة العصبية الاصطناعية.

1. INTRODUCTION

The global transition to renewable energies is changing how we produce and use energy. As countries aim to reduce greenhouse gas emissions, they are increasingly turning to cleaner energy solutions. Hydrogen has become a promising energy source due to its clean-burning nature and high energy content, particularly valuable in industries and transportation sectors where direct electrification is challenging [1], [2]. However, for hydrogen to be truly sustainable, its production must also be efficient and environmentally friendly. One effective method for producing hydrogen is through Proton Exchange Membrane (PEM) water electrolysis powered by sources of renewable energy such as solar energy. Laghlimi et al. (2024) explores the historical evolution and modern techniques of green hydrogen production through water electrolysis, highlighting its role in sustainable energy. It emphasizes environmentally friendly methods for addressing the challenges of climate change [3]. Solar photovoltaic (PV) systems, which take advantage of the sun's energy, are widely used due to their reliability and availability [4]. Nevertheless, the integration of PV systems with PEM electrolyzers poses significant challenges, as solar energy varies throughout the day, causing fluctuations in the power generated [5]. These fluctuations can have an impact on the performance of PEM electrolyzers, which require a stable power supply to produce hydrogen efficiently [6]. Consequently, solving these problems requires advanced systems to efficiently manage and control the flow of energy [7]. Various techniques have been applied to meet the challenges of integrating photovoltaic systems with PEM electrolyzers [8]. Traditional control methods, such as proportional-integral (PI) and proportional-integral-derivative (PID) controllers, are widely utilized because they are straightforward and simple to implement [9]. These methods can effectively control voltage and current under stable, predictable conditions. However, their performance decreases when confronted with highly variable solar irradiation or rapid environmental changes, as they suffer from a lack of adaptability and may encounter nonlinear system behavior [10]. Advanced control strategies such as fuzzy logic and model predictive control (MPC) have also been investigated for their ability to handle non-linearity and variability [11], but these approaches often require significant computational resources and may be less effective at adapting to dynamic conditions over time [12]. In contrast, artificial neural networks (ANNs) are a promising alternative, offering significant advantages in complex, dynamic systems [13]. ANNs can model non-linear relationships, learn from data and adapt to changing input

conditions, making them particularly well suited to renewable energy applications [14]. Unlike traditional methods, ANNs do not depend on predefined system models, enabling them to deal more effectively with variability and unpredictability. This study exploits the adaptive and learning capabilities of ANNs to improve the stability and performance of the integrated PV-PEM system, addressing the limitations of conventional techniques [15]. This research proposes an artificial neural network (ANN)-based control approach to improve the efficiency and stability of proton exchange membrane (PEM) water electrolysis when powered by a photovoltaic (PV) system under variable sunlight conditions. The inherent intermittency of solar energy leads to voltage and current fluctuations that can have a negative impact on electrolyzer performance, reducing hydrogen production efficiency and increasing stress on system components. To mitigate these issues, the proposed system incorporates maximum power point tracking (MPPT) using the Perturb and Observe (P and O) algorithm, which continuously adjusts the operating point of the photovoltaic array to extract the maximum available power [16]. A boost converter raises the photovoltaic voltage to an appropriate level for efficient energy conversion, while a buck converter precisely regulates the voltage supplied to the electrolyzer, ensuring optimal operating conditions for hydrogen production [17], [18]. At the heart of the proposed approach is an ANN-based control system that dynamically adapts to rapid changes in solar irradiance and temperature, enabling more efficient and stable power regulation compared to traditional proportional-integral (PI) control. Unlike fixed-parameter controllers, the ANN is trained to recognize complex patterns in power fluctuations and adjust control signals accordingly, improving voltage stability and reducing energy losses [19]. The performance of the ANN-based controller is rigorously evaluated by comparing it with conventional PI control in terms of hydrogen production efficiency, voltage stability and overall system reliability.

The results of this study demonstrate that the ANN-based control approach significantly improves electrolyzer efficiency and durability, ensuring constant hydrogen production even under fluctuating solar energy conditions. This research contributes to the development of intelligent control strategies for electrolysis systems powered by renewable energies, paving the way for more sustainable, resilient and efficient hydrogen production technologies.

2. SYSTEM DESCRIPTION AND DESIGN

2.1. The Electrical Equivalent Representation of the PEM Electrolyzer

Our system consists of a photovoltaic hydrogen production setup that includes a solar panel, a boost converter for MPPT, and a buck converter to step down the voltage to 7.5V. This configuration powers a 400W PEM electrolyzer for efficient hydrogen generation, as shown in Figure 1.

The design parameters for the PEM electrolyzer, solar panel, boost converter, and buck converter are outlined in the following subsections.

The electrical equivalent model of the PEM electrolyzer is an essential tool for testing and validating the performance of control techniques and power topologies. It provides a robust method for simulating electrolyzer behavior without the need for physical hardware implementation, thus mitigating risks such as damage caused by voltage overshoot and current ripple.

Various electrical models of PEM electrolyzers have been proposed in the literature. Some studies, such as references [20], [21], represent the electrolyzer as a simple resistor. Others, including references [22], [23], model it using an equivalent electrical circuit made up of a resistor (R_{elz}) and a reversible voltage (E_{elz}) connected in series. This approach captures the electrolyzer's static electrical characteristics, such as its voltage, current, and power-current relationships.

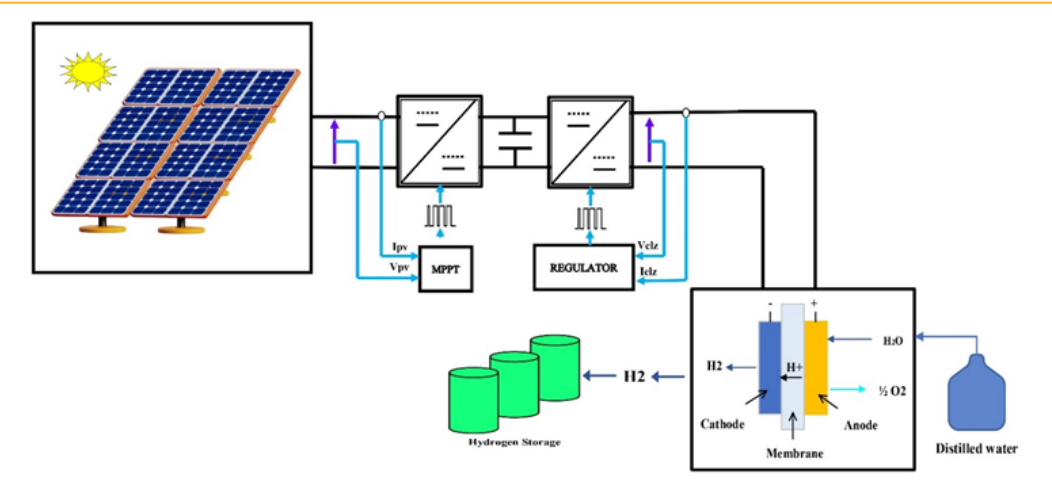


Figure 1 Schematic Representation of the Discussed System.

In this study, the PEM electrolyzer is represented as a series combination of a resistor and a reversible DC voltage. This model provides an accurate representation of the electrolyzer's operating range and behavior, expressed in the following mathematical equation (1.1):

$$V_{elz} = R_{elz}I_{elz} + E_{elz} = 0.0625I_{elz} + 4.375$$
 (1.1)

The electrical behavior in the range of 3A to 50A can be approximated through linear interpolation to determine the coefficients of this equation (1.1) [24]. The experimental data, sourced from [24] demonstrates a nearly linear relationship between voltage and current, as depicted in Fig. 2. This observation lends credence to the idea that the system can be modeled using resistances and a reversible voltage.

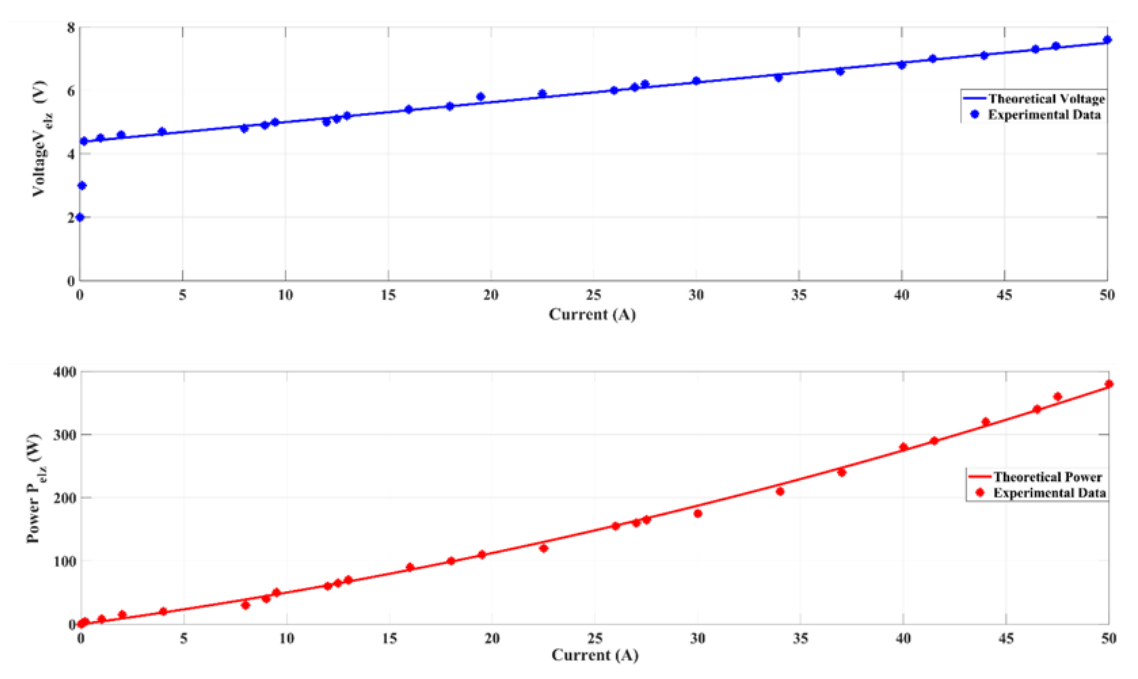


Figure 2 Static characteristics of the selected PEM electrolyzer cells.

The method for determining the hydrogen production rate (N_{H_2}) in moles per second, is presented in equation (1.2), where n is the number of electrons involved, I is the electric current in amperes, and F is Faraday's constant (96485 C/mol)}.

$$N_{H_2} = \frac{nI}{2F} \quad (\text{ moles / s})$$
 (1.2)

The hydrogen produced can be transformed from moles per second to liters per minute using the following equation (1.3):

$$N_{H_2} = 0.00696nI \quad (L/min)$$
 (1.3)

Table 1 PEM Electrolyzer Specifications.

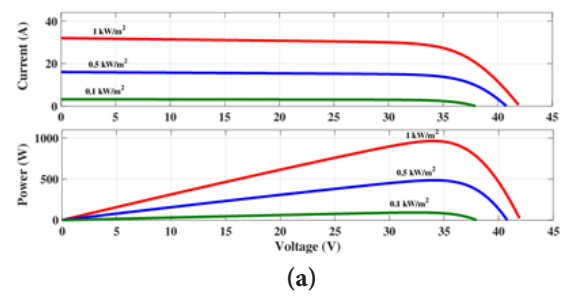
Specification	Result	
Rated Electrolyzer Power	400	Watts
Stack Operating Electrolyzer Voltage	2.28	Volts
Stack Electrolyzer Current	0 50	Amperes
Output Pressure.	0.110.5	bar
Hydrogen Flow Rate at Standard Temperature and Pressure	1	Litre/min
Cell Numbers	3	-

2.2. Solar Photovoltaic Array

Solar photovoltaic units are arranged in parallel and series to increase power output and form solar photovoltaic arrays. The solar panel discussed in this article consists of two panels connected in series and four panels connected in parallel. Together, these panels have a total maximum power capacity of 965.6 W, as shown in Figure 2. The specifications of the solar modules are provided in Table 2.

Table 2 Solar panel parameters for Waaree Energies WU-120.

Parameters	Value
\mathbf{I}_{mp}	7.1 A
\mathbf{V}_{mp}	17 V
P _{max,e}	120.7 W
\mathbf{I}_{sc}	8 A
\mathbf{V}_{oc}	21 V
PV solar irradiation (G)	1000 W/m ²
PV operation temperature (T)	25 °C



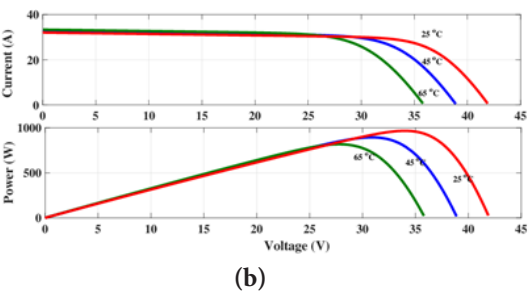


Figure 3 Voltage-current and voltage-power characteristics of a photovoltaic panel (Waare Energies WU-120, 2 series modules, 4 parallel strings) (a) for different irradiance levels (G) at T = 25°C; (b) for different temperatures

with
$$G = 1000 \ W / m^2$$

2.3. Boost Converter

A boost converter, as shown in Figure 4, is employed for MPPT operation. Its input is the peak voltage of the solar panel, with the MPP voltage fixed at 34V. The output of the boost converter is represented by the DC link voltage (V_{mppt}), which is set at 50V. The duty cycle D_{pv} , inductance

 L_{pv} , and capacitor Cpv of the boost converter are determined using the following equations (1.4):

$$D_{pv} = \frac{V_{mppt} - V_{pv}}{V_{mppt}} \tag{1.4}$$

$$L_{pv} = \frac{V_{pv}D_{pv}}{f_{s_{pv}}\Delta I_{pv}} \tag{1.5}$$

$$C_{pv} = \frac{I_{pv}}{f_{s_{mv}} \Delta V_{pv}} \tag{1.6}$$

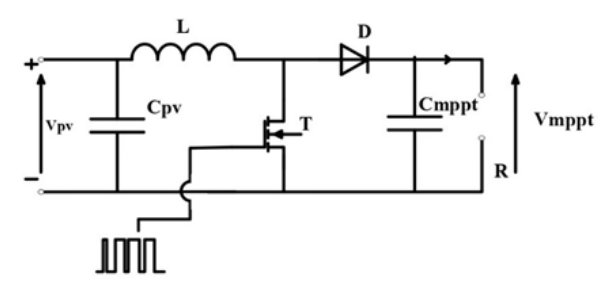


Figure 4. Electrical schematic of the DC-DC Boost converter.

Table 3 MPPT boost parameters [25].

Parameters	Values
Boost Input Voltage (V_{pv})	42V
Boost Output Voltage (V_{mppt})	50V
Inductor (L_{pv})	0.5 mH
Input capacitor (C_{pv})	1000μF
Output capacitor (C_{mppt})	1600μF
Switching Frequency (f_{spv})	10 kHz

2.4. Buck Converter

Electrolyzers typically require a low DC voltage for water electrolysis, which is why a DC/DC buck converter, as shown in Figure 5, is often used. These converters not only reduce the voltage but also perform voltage conditioning, owing to the non-linear voltage characteristics of the electrolyzer stack. The parameters of the buck converter are calculated as follows:

$$D_{elz} = \frac{V_{elz}}{V_{mont}} \tag{1.7}$$

$$L_{elz} = \frac{V_{elz}(1 - D_{elz})}{f_{s_{elz}} \Delta I_{elz}}$$
 (1.8)

$$C_{elz} = \frac{V_{elz}(1 - D_{elz})}{8L_{elz}f_{s_{ol}}^2 \Delta V_{elz}}$$
(1.9)

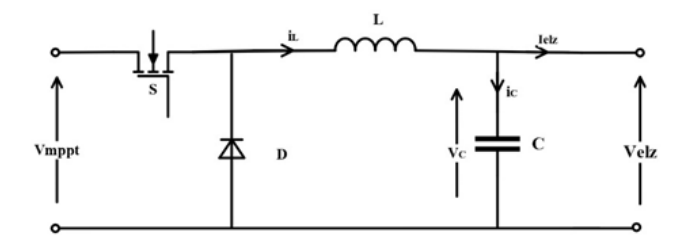


Figure 5. Electrical schematic of the DC-DC Buck converter.

Table 4 Specification of the Buck converter [25].

Parameters	Values
Buck Input Voltage (V_mppt)	50V
Buck Output Voltage (V_elz)	7.5V
Inductor (L_elz)	1.5 mH
Capacitor (C_elz)	100μF
Switching Frequency (f_sel)	10 kHz

3. CONTROL STRATEGIES

The electrical control strategy for the selected system uses two controllers: perturbation and observation (P&O) for maximum power point tracking (MPPT) and a proportional-integral (PI) controller. We replace the PI controller with an artificial neural network (ANN)-based control to compare their performance. Each controller is adapted to specific functions, working together to optimize system performance, ensure stability, and improve reliability.

3.1. MPPT Controller

The MPPT controller regulates the boost converter to maximize power extraction from the solar panel. The perturbation and observation (P&O) technique, shown in Figure 6, is employed as the MPPT algorithm due to its simplicity and broad practical use [26]

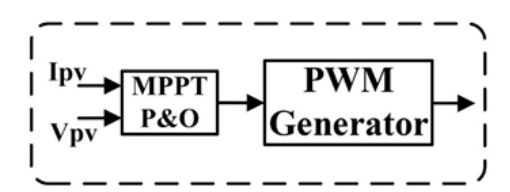


Figure 6. System Electrical Control Strategy using MPPT (P and O).

3.2. PI Controller

A proportional-integral (PI) controller Figure 7 is implemented to regulate the buck converter, ensuring that the output voltage supplied to the electrolyser remains stable. The PI controller evaluates the difference between the reference voltage and the actual voltage, generating the control signal for pulse-width modulation (PWM) to adjust the buck converter's duty cycle.

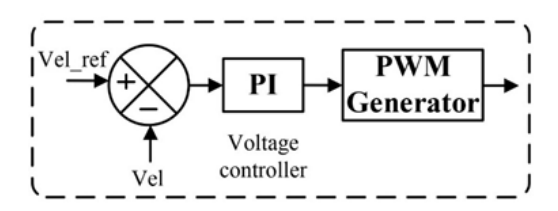


Figure 7. System Electrical Control Strategy using PI Controller.

3.3. ANN-based Controller

For our model Figure 8, we use 64 hidden neurons and the Levenberg-Marquardt learning algorithm. The data collected to train the ANN model includes the error between the desired value (7.5 V) and the actual output voltage, as well as the error variation , which indicates the variation in the error signal between successive time steps. In addition, the previous control output D is used as an input that reflects the control signal generated by the PI controller during the previous time step. The output of the model is the current output of the PI controller, which serves as a duty cycle sent to the PWM generator to convert it into a PWM signal for the power converter.

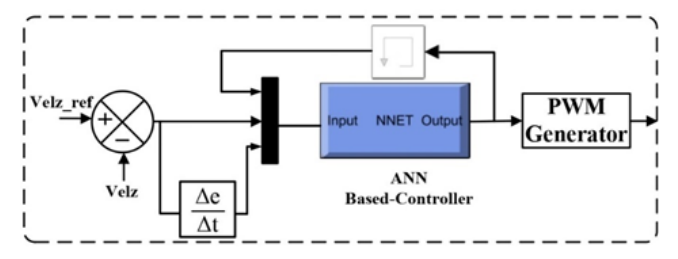


Figure 8. System Electrical Control Strategy using ANN Based-Controller.

4. RESULTS AND DISCUSSION

The dynamic performance of the system under varying atmospheric conditions is illustrated by data recorded in our laboratory. These results reflect the system's behavior under fluctuating solar irradiation and temperature conditions. Solar irradiance varies from 400 W/m² to 1000 W/m², while the temperature of the photovoltaic panel fluctuates between 42°C and 62°C, as shown in Figure 9(a) and Figure 9(b), respectively. These variations have a direct impact on PV system parameters such as PV voltage (V_{pv}) and power (p_{pv}), illustrated in Figure 9(c) and Figure 9(d) respectively. The irradiance curve Figure 9(b) first shows a steady increase, which is followed by a sharp decrease near the mid-point, corresponding to a temporary drop in solar irradiance. This reduction in irradiance is reflected in the PV voltage profile Figure 9(c). Power output (p_{pv}) Figure 9(d) also follows a similar pattern, fluctuating with irradiation and temperature changes, as well as with other system parameters.

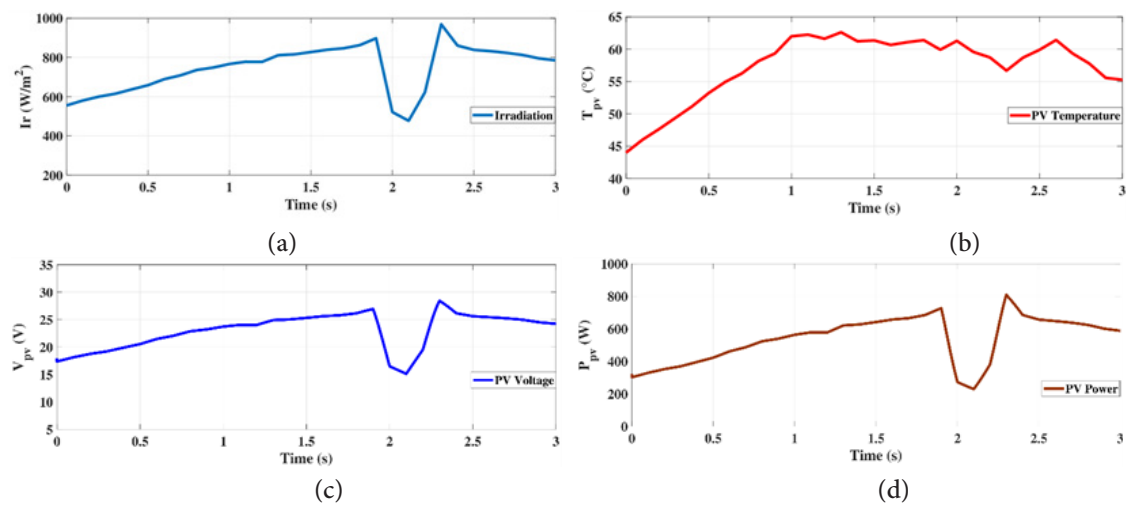


Figure 9. Dynamic performance of the system with varying solar irradiation and Temperature, where Solar irradiance, (b) Temperature of the photovoltaic panel, (c) PV voltage (V_{pv}) and (d) Power output (p_{pv}) .

The Figure 10 shows how a photovoltaic (PV) system behaves under MPPT control. In Figure 10(a), the PV voltage (V_{PV}) and the MPPT voltage (V_{PPT}) are stable after an initial transient, but

a dip is visible around 2 seconds before the system recovers. Figure 10(b) focuses on the current response, where both the PV current (I_{PV}) and MPPT current (I_{MPPT}) experience a spike during the same disturbance. Figure 10(c) provides a closer look at the power response during steady-state and disturbance periods. Overall, the figure highlights how the system manages initial transients, maintains steady-state operation, and effectively responds to external disturbances.

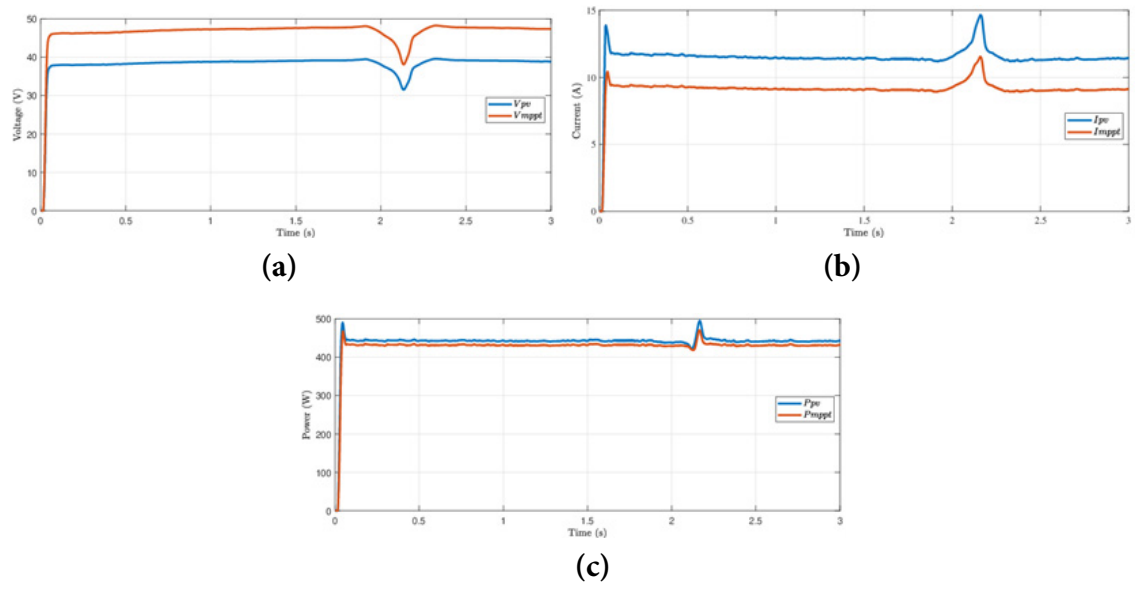


Figure 10. Dynamic Response of a Photovoltaic System Under MPPT Control where (a) the PV voltage (V_{pv}) and the MPPT voltage (M_{PPT}), (b) the PV current (I_{pv}) & MPPT current (I_{mppt}) and (b) the PV Power (P_{pv}).

This Figure 11 compares the performance of a Proportional-Integral (PI) controller and an Artificial Neural Network (ANN) controller in regulating an electrolyzer system.

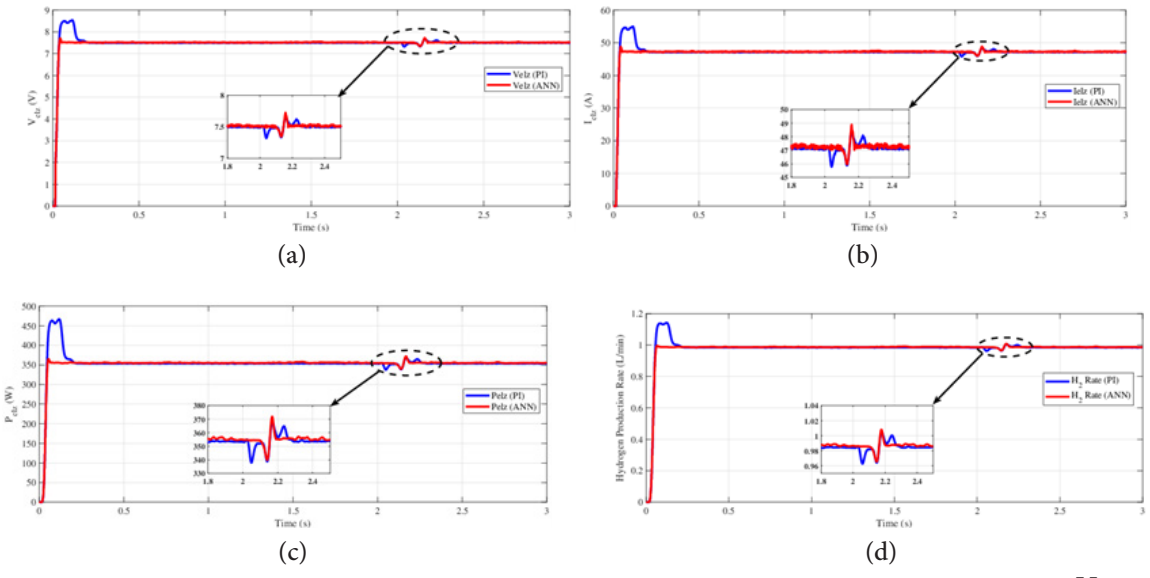


Figure 11. Dynamic performance of the system with varying solar irradiation (a) the voltage response (V_{elz}), (b) The current response (I_{elz}) (c) the power output (P_{elz}) and (d) the hydrogen production rate (Rate) all under PI and ANN control.

Figure 11(a) shows the voltage response(V_{elz}), where the ANN controller achieves faster stabilization and smoother behavior after a disturbance at around 2 seconds, while the PI controller shows more pronounced oscillations. In Figure 11(b), the current response (I_{elz}) is

displayed, with the ANN controller providing a more stable and consistent response, effectively suppressing fluctuations during the disturbance. Figure 11(c) focuses on the power output (P_{elz}), where the ANN controller demonstrates quicker recovery and steadier performance under transient and steady-state conditions compared to the PI controller.

Finally, Figure 11(d) presents the hydrogen production rate (H₂ Rate), highlighting the ANN controller's ability to maintain a more stable and reliable output, even during disturbances. Overall, the result shows that the ANN controller outperforms the PI controller, delivering faster responses, better stability, and improved efficiency under varying operating conditions.

The results Table 5 demonstrate that the ANN controller outperforms the PI controller on several performance parameters. The ANN has a minimum overshoot of 3.1%, significantly lower than the PI's 12.84%, indicating a more controlled and consistent response close to the target value. In terms of settling time, the PI controller has a settling time of 0.023 s, while the ANN stabilizes at 0.022 s. In addition, the PI controller's mean absolute percentage error MAPE is 1.22%, while the ANN achieves a lower MAPE of 0.95%, indicating improved tracking accuracy. Overall, these parameters suggest that the ANN controller performs better than the PI controller in terms of tracking accuracy. In addition, the average flow rates for hydrogen production are 0.98 L/min for the PI controller and 0.99 L/min for the ANN controller, indicating that the ANN performs better in terms of hydrogen production efficiency.

Table 5 Dynamic Performance o	f Controllers.
-------------------------------	----------------

Controller	MAPE (%)	Settling Time (S)	Overshoot (%)
PI	1.22	0.023	12.84
ANN	0.95	0.022	3.19

5. CONCLUSIONS

In this study, we investigated a system integrating a PEM water electrolyzer and a photovoltaic panel to address the challenges of hydrogen production under fluctuating solar energy conditions. The system uses a boost converter with a perturbation and observation P&O algorithm for MPPT and a buck converter to stabilize the voltage supplied to the electrolyzer. Initially, the buck converter was controlled using a PI strategy, but to address the limitations caused by the system's non-linearity, we proposed the use of an ANN controller. The results indicated that the ANN controller outperformed the PI controller in terms of stability and overall system performance. The ANN achieved 3.19% less overshoot} than the PI's 12.84 %, 0.022 s faster stabilization than the PI's 0.023 s, and 0.95% less mean absolute percentage error (MAPE) than the PI's 1.22%. In addition, hydrogen production rates were higher with the ANN (0.99 L/min vs. 0.98 L/min for the PI). Future work could explore advanced ANN techniques, such as deep learning and reinforcement learning, to improve system accuracy and adaptability, even in the presence of different disturbances. In addition, the integration of improved converters and MPPT strategies can maximize energy extraction and system efficiency, contributing to the sustainability of the electrolyzer and the advancement of sustainable green hydrogen production.

Authors contribution: Abdellah EL IDRISSI / developed the concept and aims of the study; Belkasem Imodane/prepared and compared the literature; Mohamed Benydir/prepared and compared the literature; Hamid Hamdani/ reviewed and checked the structure of the manuscript; M'hand Oubella/ reviewed and checked the structure of the manuscript; Mohamed Ajaamoum/ reviewed and checked the structure of the manuscript.

All authors contributed to the final manuscript.

All authors have read and approved the manuscript.

Funding: The article is supported by the The Moroccan Association of Sciences and Techniques for Sustainable Development (MASTSD), Beni Mellal, Morocco.

Data Availability Statement: The data supporting the findings of this study are available upon reasonable request from the corresponding author.

Conflicts of Interest: The authors declare that there is no conflict of interest regarding the publication of this paper.

Acknowledgements: Authors may acknowledge any person, institution, or department that supported any part of the study.

REFERENCES

- [1] Q. Hassan, S. Algburi, A. Z. Sameen, H. M. Salman, and M. Jaszczur, "Green hydrogen: A pathway to a sustainable energy future," Int J Hydrogen Energy, vol. 50, pp. 310–333, 2024, doi: https://doi.org/10.1016/j.ijhydene.2023.08.321.
- [2] B. Reda, A. A. Elzamar, S. AlFazzani, and S. M. Ezzat, "Green hydrogen as a source of renewable energy: a step towards sustainability, an overview," Environ Dev Sustain, May 2024, doi: 10.1007/s10668-024-04892-z.
- [3] C. Laghlimi, A. Moutcine, Y. Ziat, H. Belkhanchi, A. Koufi, and S. Bouyassan, "Hydrogen, Chronology and Electrochemical Production," JSESD, pp. 22–37, Dec. 2024, doi: https://doi.org/10.51646/jsesd.v14iSI MSMS2E.405.
- [4] D. Mazumdar, C. Sain, P. K. Biswas, P. Sanjeevikumar, and B. Khan, "Overview of solar photovoltaic MPPT methods: a state of the art on conventional and artificial intelligence control techniques," International Transactions on Electrical Energy Systems, vol. 2024, no. 1, p. 8363342, 2024, Accessed: Apr. 03, 2025. [Online]. Available: https://doi.org/10.1155/2024/8363342
- [5] Y. Astriani, W. Tushar, and M. Nadarajah, "Optimal planning of renewable energy park for green hydrogen production using detailed cost and efficiency curves of PEM electrolyzer," Int J Hydrogen Energy, vol. 79, pp. 1331–1346, 2024, Accessed: Apr. 03, 2025. [Online]. Available: https://doi.org/10.1016/j.ijhydene.2024.07.107
- [6] C. Yan, Y. Zou, Z. Wu, and A. Maleki, "Effect of various design configurations and operating conditions for optimization of a wind/solar/hydrogen/fuel cell hybrid microgrid system by a bioinspired algorithm," Int J Hydrogen Energy, vol. 60, pp. 378–391, 2024, Accessed: Apr. 03, 2025. [Online]. Available: https://doi.org/10.1016/j.ijhydene.2024.02.004
- [7] F. S. Al-Ismail, "A critical review on DC microgrids voltage control and power management," IEEE Access, 2024, doi: 10.1109/ACCESS.2024.3369609.
- [8] V. A. M. Lopez, H. Ziar, J. W. Haverkort, M. Zeman, and O. Isabella, "Dynamic operation of water electrolyzers: A review for applications in photovoltaic systems integration," Renewable and Sustainable Energy Reviews, vol. 182, p. 113407, 2023, Accessed: Apr. 03, 2025. [Online]. Available: https://doi.org/10.1016/j.rser.2023.113407
- [9] Z. Han, X. Yao, S. Yuan, H. Dong, S. Ma, and Y. Dong, "Research on control strategy of photovoltaic hydrogen generation system based on Fuzzy PI control," Energy Reports, vol. 9, pp. 4187–4194, 2023, doi: https://doi.org/10.1016/j.egyr.2023.02.079.
- [10] M. Khalid, "Smart grids and renewable energy systems: Perspectives and grid integration challenges," Energy Strategy Reviews, vol. 51, p. 101299, 2024, Accessed: Apr. 03, 2025. [Online]. Available: https://doi.org/10.1016/j.esr.2024.101299
- [11] Z. Wei, P. W. Tien, J. Calautit, J. Darkwa, M. Worall, and R. Boukhanouf, "Investigation

- of a model predictive control (MPC) strategy for seasonal thermochemical energy storage systems in district heating networks," Appl Energy, vol. 376, p. 124164, 2024, Accessed: Apr. 03, 2025. [Online]. Available: https://doi.org/10.1016/j.apenergy.2024.124164
- [12] L. Wang et al., "An integrated deep learning model for intelligent recognition of long-distance natural gas pipeline features," Reliab Eng Syst Saf, vol. 255, p. 110664, 2025, Accessed: Apr. 03, 2025. [Online]. Available: https://doi.org/10.1016/j.ress.2024.110664
- [13] S. A. Kalogirou, "Applications of artificial neural networks in energy systems," Energy Convers Manag, vol. 40, no. 10, pp. 1073–1087, 1999, doi: https://doi.org/10.1016/S0196-8904(99)00012-6.
- [14] L. Nolting, T. Spiegel, M. Reich, M. Adam, and A. Praktiknjo, "Can energy system modeling benefit from artificial neural networks? Application of two-stage metamodels to reduce computation of security of supply assessments," Comput Ind Eng, vol. 142, p. 106334, 2020, doi: https://doi.org/10.1016/j.cie.2020.106334.
- [15] M. Abdelkareem et al., "Progress of artificial neural networks applications in hydrogen production," Chemical Engineering Research and Design, vol. 182, Mar. 2022, doi: 10.1016/j. cherd.2022.03.030.
- [16] L. Zou, Q. Shen, G. Yang, S. Li, and N. Huang, "Improved hydrogen production efficiency of a Photovoltaic-Electrolysis system with P&O Algorithm: A case study," Chem Phys Lett, vol. 832, p. 140891, 2023, doi: https://doi.org/10.1016/j.cplett.2023.140891.
- [17] A. Hassan, O. Abdel-Rahim, M. Bajaj, and I. Zaitsev, "Power electronics for green hydrogen generation with focus on methods, topologies, and comparative analysis," Sci Rep, vol. 14, no. 1, p. 24767, 2024, Accessed: Apr. 03, 2025. [Online]. Available: https://doi.org/10.1038/s41598-024-76191-6
- [18] M. A. Hossain, M. R. Islam, M. A. Hossain, and M. J. Hossain, "Control strategy review for hydrogen-renewable energy power system," J Energy Storage, vol. 72, p. 108170, 2023, Accessed: Apr. 03, 2025. [Online]. Available: https://doi.org/10.1016/j.est.2023.108170
- [19] S. Adiche et al., "Advanced control strategy for AC microgrids: a hybrid ANN-based adaptive PI controller with droop control and virtual impedance technique," Sci Rep, vol. 14, no. 1, p. 31057, 2024, Accessed: Apr. 03, 2025. [Online]. Available: https://doi.org/10.1038/s41598-024-82193-1
- [20] M. E. Şahin, H. İ. Okumuş, and M. T. Aydemir, "Implementation of an electrolysis system with DC/DC synchronous buck converter," Int J Hydrogen Energy, vol. 39, no. 13, pp. 6802–6812, 2014, doi: https://doi.org/10.1016/j.ijhydene.2014.02.084.
- [21] B. Yodwong, D. Guilbert, W. Kaewmanee, and M. Phattanasak, "Energy Efficiency Based Control Strategy of a Three-Level Interleaved DC-DC Buck Converter Supplying a Proton Exchange Membrane Electrolyzer," Electronics (Basel), vol. 8, no. 9, 2019, doi: 10.3390/electronics8090933.
- [22] M. Albarghot and L. Rolland, "Comparison of experimental results with simulation of a PEM Electrolyzer powered by a horizontal wind turbine," in 2017 International Conference of Electrical and Electronic Technologies for Automotive, 2017, pp. 1–6. doi: 10.23919/EETA.2017.7993232.
- [23] S. M. Muyeen, R. Takahashi, and J. Tamura, "Electrolyzer switching strategy for hydrogen generation from variable speed wind generator," Electric Power Systems Research, vol. 81, no. 5, pp. 1171–1179, 2011, doi: https://doi.org/10.1016/j.epsr.2011.01.005.
- [24] F. Alonge, S. M. Collura, F. D'Ippolito, D. Guilbert, M. Luna, and G. Vitale, "Design of a robust controller for DC/DC converter—electrolyzer systems supplied by µWECSs subject to highly fluctuating wind speed," Control Eng Pract, vol. 98, p. 104383, 2020, doi: https://doi.org/10.1016/j.conengprac.2020.104383.

- [25] R. K. Kumar and P. Samuel, "Designing a hydrogen generation system through PEM water electrolysis with the capability to adjust fast fluctuations in photovoltaic power," Int J Hydrogen Energy, vol. 82, pp. 1–10, 2024, Accessed: Apr. 03, 2025. [Online]. Available: https://doi.org/10.1016/j.ijhydene.2024.07.376
- [26] S. D. Al-Majidi, M. F. Abbod, and H. S. Al-Raweshidy, "A novel maximum power point tracking technique based on fuzzy logic for photovoltaic systems," Int J Hydrogen Energy, vol. 43, no. 31, pp. 14158–14171, 2018, Accessed: Apr. 03, 2025. [Online]. Available: https://doi.org/10.1016/j.ijhydene.2018.06.002

List of Abbreviations:

Abbreviation	Meaning
ANN	Artificial Neural Network
DC	Direct Current
MAPE	Mean Absolute Percentage Error
MPPT	Maximum Power Point Tracking
P&O	Perturbation and Observation (MPPT algorithm)
PEM	Proton Exchange Membrane
PI	Proportional-Integral (Control)
PV	Photovoltaic

Nomenclature:

Symbol	Meaning
H_2	Hydrogen Gas
I_{elz}	Electrolyzer Current (A)
I_{mppt}	Maximum Power Point Tracking Current (A)
I_r	Irradiance (W/m²)
I_{pv}	Photovoltaic Current (A)
N_{h2}	Hydrogen Production Rate (moles/s or L/min)
P_{elz}	Electrolyzer Power (W)
P_{mppt}	Maximum Power Point Tracking Power (W)
P_{pv}	Photovoltaic Power (W)
T_{pv}	Photovoltaic Temperature (°C)
V_{elz}	Electrolyzer Voltage (V)
V_{mppt}	Maximum Power Point Tracking Voltage (V)
V_{pv}	Photovoltaic Voltage (V)